https://doi.org/10.5194/egusphere-2025-6391
Preprint. Discussion started: 30 December 2025

Effects of convective intensity and organisation on the structure and lifecycle of deep convective clouds

William K. Jones[1] and Philip Stier[1]

[1]Atmospheric, Oceanic and Planetary Physics, Department of Physics, University of Oxford

Correspondence: William K. Jones (william.jones@physics.ox.ac.uk)

Abstract. The structure of anvil clouds is important for their effects on the climate, as the net radiative effect depends on the balance of thick and thin areas. Recent studies have shown an important, warming feedback to climate change due to the thinning of anvils, however there is no clear mechanism behind these observed changes. Previous studies have shown a relationship between the intensity of convection and the proportion of thin anvil. In this study, we use cloud tracking approach with geostationary satellite observations to relate changes in anvil properties to convective intensity and organisation over their entire lifecycle. We find that while increasing intensity of convection is linked to an increase in the proportion of thin anvil, increasing organisation has no effect. Furthermore, these two convective processes also have contrasting effects on the lifecycle of anvil clouds. As the albedo response depends on changes in anvil structure, differences in convective regimes which prefer either organised or isolated but intense convection may lead to regional differences in anvil feedbacks. We propose that the anvil structure response is a combination of effects from the impact of convective intensity on initial anvil formation and changes in anvil dissipation rate due to effects on sedimentation rates and sublimation rates from changes in the anvil environment. Understanding each of these processes and their relative impacts is vital to understanding the future response of anvil structure to climate change.

1 Introduction

Understanding how the structure of anvil clouds changes in response to changes in convective behaviour is vital to understanding the radiative impacts and climate feedbacks of deep convective clouds (DCCs). Around 50% of cirrus clouds in the tropics originate from deep convection (Massie et al., 2002; Luo and Rossow, 2004). Overall, anvil clouds have a near-neutral radiative impact on the tropics, despite their large shortwave (SW) reflectance and longwave (LW) absorption (Hartmann et al., 1992; Hartmann, 2016). Their radiative effect is not homogeneous however; while the optically thick portion of anvil clouds generally have a cooling effect on the top-of-atmosphere (ToA) radiative balance, the thin, detrained cirrus has a strong warming effect (Berry and Mace, 2014). As a result, changes in convective activity that result in a change in the size and structure of anvil clouds may have large impacts on the climate.

https://doi.org/10.5194/egusphere-2025-6391
Preprint. Discussion started: 30 December 2025

The change of anvil cloud area in response to warming—the iris effect (Lindzen et al., 2001; Bony et al., 2016)—is generally considered to have a cooling feedback in response to climate change. However, it is the largest source of uncertainty in cloud–climate feedbacks, with around a third of models predicting a warming response (Sherwood et al., 2020). Recent research has shown evidence for an anvil thinning response to warming both in observations (Raghuraman et al., 2024) and high-resolution models (Sokol et al., 2024), in which the reduction in anvil cloud albedo results in a warming feedback opposing and cancelling out that from the area feedback. This anvil thinning response, however, shows large variance between models, and there are few constraints on changes in anvil cloud albedo (McKim et al., 2024). Impacts on anvil cloud albedo from changes in convective organisation (Bony et al., 2020) may account for some of this uncertainty. To address this uncertainty, a better understanding of the links between convective processes and anvil properties, changes in anvil structure and the properties of ice clouds are required (Gasparini et al., 2023).

Assessing the extent of thin anvil cirrus is challenging due to the difficulties in observing these clouds using infrared (IR) radiometers. The low emissivity of thin cirrus clouds means that observed brightness temperature (BT) is dominated by radiances from the lower atmosphere and surface below. Protopapadaki et al. (2017) used cloud emissivity and cloud top pressure, rather than BT, to detect convective cores, thick and thin anvil cirrus clouds. Data from the atmospheric infrared sounder (AIRS) was used to retrieve these emissivity values, as the hyperspectral sounder is more sensitive to thin cirrus than IR radiometers. They then compared the proportion of each anvil cloud consisting of thin anvil to the minimum observed cloud top temperature within the convective core, a proxy for the convective depth which is, in turn, a proxy for convective intensity. It was found that the thin cirrus anvil proportion increased with colder cloud top temperatures, indicating that stronger convection increases the detrainment of thin cirrus. Takahashi et al. (2017) built upon this study using collocated measurements from the cloud profiling radar aboard CloudSat. These measurements provide the echo top height, measuring the convective depth directly, and also provide another proxy for convective intensity, the echo top distance, which is independent of convective depth (Takahashi and Luo, 2014). It was again found that the proportion of thin cirrus increased with the echo top height, and also increased with decreasing echo top distance (indicating stronger convection).

It should be noted that both of these studies were performed using observations from polar-orbiting satellites in the A-train, and so do not fully sample the diurnal cycle. While both studies consider the maturity of the DCCs observed, the thin anvil proportion is measured at a single point in time, and so differences in the lifetime of the thick and thin anvil cirrus are not considered. Furthermore, we should expect that the structure of the anvil changes over its lifetime, with the thin anvil fraction increasing as the anvil dissipates. However, the observed BT of the anvil also changes over its lifetime (Futyan and Del Genio, 2007), and so the use of BT as a proxy for convective intensity may introduce confounding factors. While the use of echo top height avoids this confounding issue, these collocated measurements can only be made when the DCC is convectively active and so cannot be used to assess the structure of dissipating anvils.

In this study, we use a Lagrangian cloud-tracking approach to investigate changes in anvil structure across their entire lifecycle. Through the detection of developing convective cores and tracking of the resultant anvil clouds, we can investigate how the intensity and organisation of the initial convection affect the properties of the anvils. Furthermore, we can also investigate

https://doi.org/10.5194/egusphere-2025-6391
Preprint. Discussion started: 30 December 2025

how these convective properties impact the lifecycle of DCCs and how the anvil structure changes across the lifetime, rather than at a single point in time.

2 Data

The modern generation of geostationary weather satellite instruments, such as the geostationary operational environment satellite (GOES)-16 advanced baseline imager (ABI) (Schmit et al., 2016), offer improved capabilities for the study of DCCs including higher spatial and temporal resolutions as well as a broad range of channels providing different insights into anvil cloud properties (Schmit et al., 2018). Using a novel cloud tracking method (Jones et al., 2023), we detect and track both growing convective cores (hereafter "cores") and their associated anvil clouds throughout their entire lifetimes. The high temporal resolution of observations made over the continental US (CONUS) domain of GOES-16 ABI allows detection of the initiating stages of convection (Henderson et al., 2021), rather than just the mature, cold anvils as tracked in older observations (e.g. Maddox (1980); Augustine and Howard (1988)). In addition, two channel combinations from ABI, the water vapour difference (WVD) and split window difference (SWD) are used to detect both thick and thin anvils.

A seven-year dataset of tracked cores and anvils, presented in Jones and Stier (2025), covering the period of 2018–2024 over the GOES-16 CONUS domain (60–120 °W, 15–50 °N) is used here to investigate how the structure of observed DCCs depends on the properties of their convective cores. Data filtering is applied to ensure every anvil in the dataset begins with a valid observed core, ensuring that the subsequent development of the anvil can be linked to the properties of the core. Furthermore, it is required that each anvil is observed for its entire lifetime, and the entire extent of both thick and thin anvil are observed over this period (i.e. the detected anvil does not intersect the edge of the domain). This results in a total of 742,134 anvils considered for analysis, which are connected to a total of 1,482,590 cores. While this does mean that fewer large anvils are considered valid as their greater extent means that they are more likely to intersect the edges of the domain (see (DeWitt and Garrett, 2024) for a deeper discussion on the impact of finite domains on measured cloud size distributions), it ensures that changes in both thick and thin anvil area can be considered robust over the entire lifecycle of the analyses anvils.

The dataset contains a range of properties relating to the observed DCCs. In this chapter, we will focus our investigations on how the area of the detected cores, thick and thin anvils change with each time step. We also analyse two related properties, which are the maximum area of the thick and thin anvil, i.e. the area at the time step when the anvil reaches its maximum observed extent, and the total area which is the sum of the areas observed at each time step over each anvils lifetime. The thin anvil proportion refers to the area of the detected thin anvil divided by the total area of both anvil and core. In general, this is calculated as the total over the entire DCC lifetime, however in section 4.4 we will investigate how this changes over the DCC lifecycle.

In addition, we consider how the BT of each core and anvil change over time. The area-weighted average of the 10.4 µm BT is taken at each time step for each core, thick and thin anvil. The 10.4 µm LW window BT has a minimal contribution from water in the atmosphere, and so can provide temperature measurements of clouds from near the surface to the top of the atmosphere. It should be noted that the BT is affected by the emissivity of the cloud, and so for thin cirrus will be warmer than

https://doi.org/10.5194/egusphere-2025-6391
Preprint. Discussion started: 30 December 2025

the actual cloud top temperature due to the contribution from the atmosphere below. As a result, we use the mean BT of the thick anvil as a proxy for convective cloud height as this avoids a bias due to the lower emissivity of the thin anvil. The cooling rate of each core is calculated as the largest (negative) change in the mean core BT measured over any 15 minute period. This relates to the vertical growth of the convective core as discussed in Jones et al. (2023), and this change in BT is correlated with intense convection measured by cloud radars (Roberts and Rutledge, 2003).

3 Method

3.1 Detection of thick and thin anvils

Observing thin cirrus anvils using satellite BT is difficult due to their low emissivity. Furthermore, BT is affected both by the height of the observed cloud and its optical thickness. As shown in fig. 1, the observed BT increases as optical depth decreases. For detection using a fixed threshold, as used in many anvil detection algorithms, this means that the limit of optical depth at which the anvil is detected increases as the height of the cloud decreases. This results in the detected anvil area varying with height, with an anvil at a lower altitude being detected as smaller than one at a higher altitude even if there size and structure are otherwise identical. This problem with detected anvil area using BT thresholds was identified as early as Augustine and Howard (1988), but remains a feature of many detection algorithms which use a fixed BT threshold for anvil detection.

While observing the thin cirrus anvil is challenging, it can be achieved by using a combination of BT differences that are sensitive to the emissivity differences of thin ice clouds. Furthermore, the use of channel differences reduces the height dependence of the detection of anvils compared to the use of a single BT. Figure 1 shows simulated BT observations using the libRadTran model (Emde et al., 2016) for ice clouds with 20 µm particle effective radius (a typical value for the top of anvil clouds (e.g. Sokol and Hartmann, 2020, fig. 8a)) across a range of optical depths at three different heights. The top panel shows simulation BT observations by ABI at 10.4 µm at heights of 10, 12 and 14 km (shown by the solid, dashed and dotted lines respectively). Also shown by the grey, dashed line is an example of the 241 K BT threshold. At this threshold there is substantial variance in the limit of cloud optical depth (COD) at which anvils are detected, which ranges from 1 at 14 km to 3 at km. This provides clear support for the argument made by Augustine and Howard (1988) that the anvil area detected using a single threshold is “subjective”.

The middle and bottom panels in fig. 1 show the simulated COD for the combinations of WVD minus SWD and WVD plus SWD, which are used for the detection of thick and thin anvils respectively. In both panels, the grey shaded region shows the BT range in which edge detection is used to find the anvil area. Compared to 10.4 µm BT, the WVD minus SWD combination shows very little variance in the optical depths at which the anvil cloud is detected within the threshold range. Throughout the threshold range of –5 to –12.5 K the COD corresponding to the same observed BT difference varies by approximately 0.1–0.2 between differing heights, compared to 1–2 for 10.4 µm BT.

The WVD plus SWD combination is shown in the bottom panel of fig. 1. Greater variance between different heights is seen, particularly for the 10 km anvil simulation. However, the COD corresponding to the observed BT differences are very similar throughout the detection range of 0 to –7.5 K for heights of 12 and 14 km. Lidar observations of thin cirrus anvil have shown

https://doi.org/10.5194/egusphere-2025-6391
Preprint. Discussion started: 30 December 2025

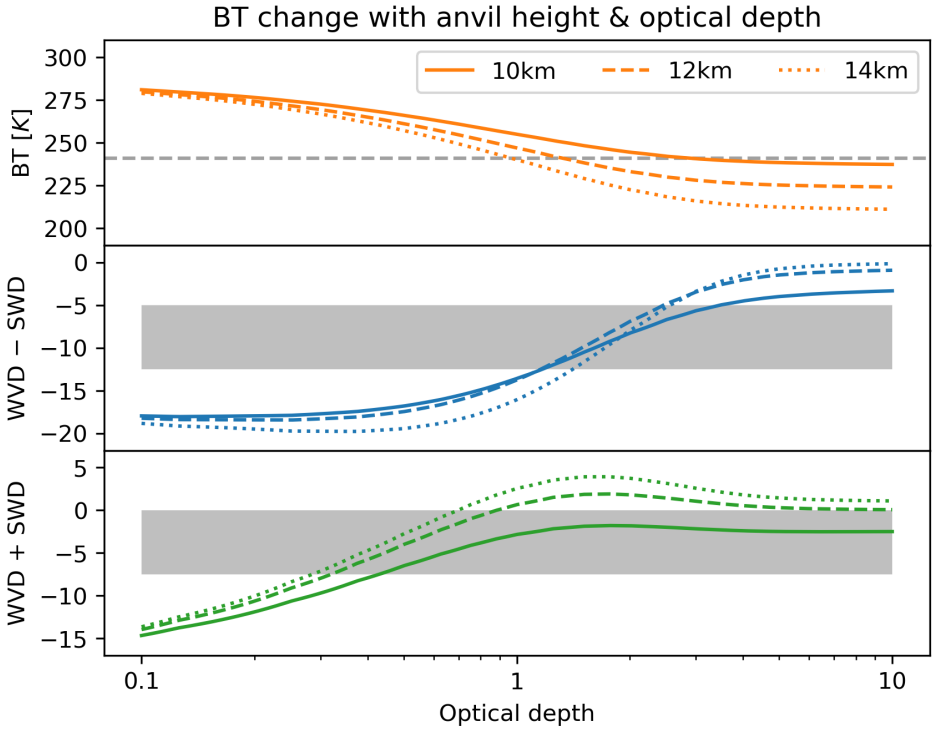

Figure 1. Simulated ABI BT observations for DCC anvils at 10 km (solid lines), 12 km (dashed lines) and 14 km (dotted lines) at optical depths between 0.1 and 10. Panels show (top) 10.4 µm BT; (middle) WVD minus SWD, used in thick anvil detection; and (bottom) WVD plus SWD, used in thin anvil detection. The grey dashed line shows the 241 [K] threshold, and the grey shaded regions show the range in which cloud edge detection is performed for thick and thin anvils.

that the heights of these clouds typically exceed 12 km (Wall et al., 2020; Horner and Gryspeerdt, 2023), and so we expect there to be little difference in the sensitivity to most observed anvils.

From fig. 1 the limits of detection for thick anvils can be estimated as 2±0.5 OD, and 0.5±0.2 OD for the thin anvil. This means that the thinnest anvil cirrus (Berry and Mace, 2014) remains undetected using this method. This may lead to biases in the calculation of the thin anvil fraction, as while all anvil thicker than the thick anvil threshold will be detected, not all the thin below the threshold will be. This could lead to an underestimate of the thin anvil area and fraction in anvils where the OD distribution shows a large frequency of very thin cirrus. Such thin anvil cirrus will have a small radiative effect on the climate, and, therefore, this bias in the thin anvil fraction may not result in a large change in the climate impacts due to the low contribution to anvil CRE from the unobserved cirrus.

It should be noted that the simulations shown in fig. 1 were calculated using a standard tropical atmospheric profile to best represent the moist environment in which deep convection occurs. While anvils occurring in the extra-tropical parts of the

https://doi.org/10.5194/egusphere-2025-6391
Preprint. Discussion started: 30 December 2025

CONUS domain are expected to have lower cloud top heights, there is also expected to be a colder temperature profile. As a result, we expect that the observed BT for extra-tropical DCCs behave more like that of the 12 and 14 km simulations shown in fig. 1, rather than that at 10 km.

3.2 Estimation of convective intensity and organisation

As we cannot observe the vertical velocity or convective mass flux of DCC updrafts directly using geostationary satellite observations, a proxy is needed to estimate their intensity instead. The minimum BT of an observed DCC is commonly used as a proxy for convective intensity, and is used by Protopapadaki et al. (2017) for this purpose. This property is more closely related to the height of the DCC, however. While the height of a DCC is related to the intensity of convection, it is also related to the tropopause height and level of neutral buoyancy which may vary with location and meteorology independent of convective processes. While we use the minimum BT of observed anvils in this chapter to compare to previous studies, a more direct proxy for convective intensity is desired.

The primary proxy for convective intensity in this chapter is the maximum cooling rate of the initial observed core for each DCC. The core cooling rate is linked to the vertical development of the core over time, as it corresponds to the change in temperature, and hence change in height, of the convective cloud envelope with the moist adiabatic lapse rate. A cooling rate of 1 $\mathrm{Kminute^{-1}}$ approximately represents a cloud top vertical velocity of 2.5 $\mathrm{ms^{-1}}$. While this should not be confused with the updraft velocity of the core itself, and is expected to be less due to the effects of entrainment and overturning circulation at the top of the updraft, it is linked to the updraft velocity directly. The initial detected core is selected for the maximum cooling rate to ensure that we have suitable observations of the core throughout its growth that are not masked by an anvil above. While the updraft may strengthen later in the development of the DCC, or subsequent cores in a multi-core system have stronger updrafts, we consider this the most direct proxy we have available for the updraft intensities of observed DCCs.

The number of cores associated with each DCC is used as a measure of its organisation, again providing the most direct proxy available. While it may not be possible to observe all the cores associated with larger mesoscale convective systems (MCSs) due to the anvil blocking observations of cores below, it is still expected that many separate cores associated with such systems are detected. Tracked DCCs with many cores tend to have much larger areas, longer lifetimes, and colder minimum BT; the expected properties of MCSs.

3.3 Lifecycle analysis

To analyse changes in the lifecycle of DCCs, we categorise their lifetime based on the method developed by Futyan and Del Genio (2007). This method separates the anvil cloud into growing, maturing and dissipating stages based on observations of BT and anvil area. Futyan and Del Genio's method defines the end of the growing phase as the time at which the anvil reaches its minimum observed BT, and the end of the mature phase as the time at which the anvil reaches the maximum observed area. While simple, this approach applies to a wide range of observed DCCs including both isolated and organised convection. Furthermore, by determining the anvil lifecycle only in terms of the observed anvil properties, we can treat the properties of the detected cores as independent variables allowing straightforward analysis of their impacts on lifecycle.

https://doi.org/10.5194/egusphere-2025-6391
Preprint. Discussion started: 30 December 2025

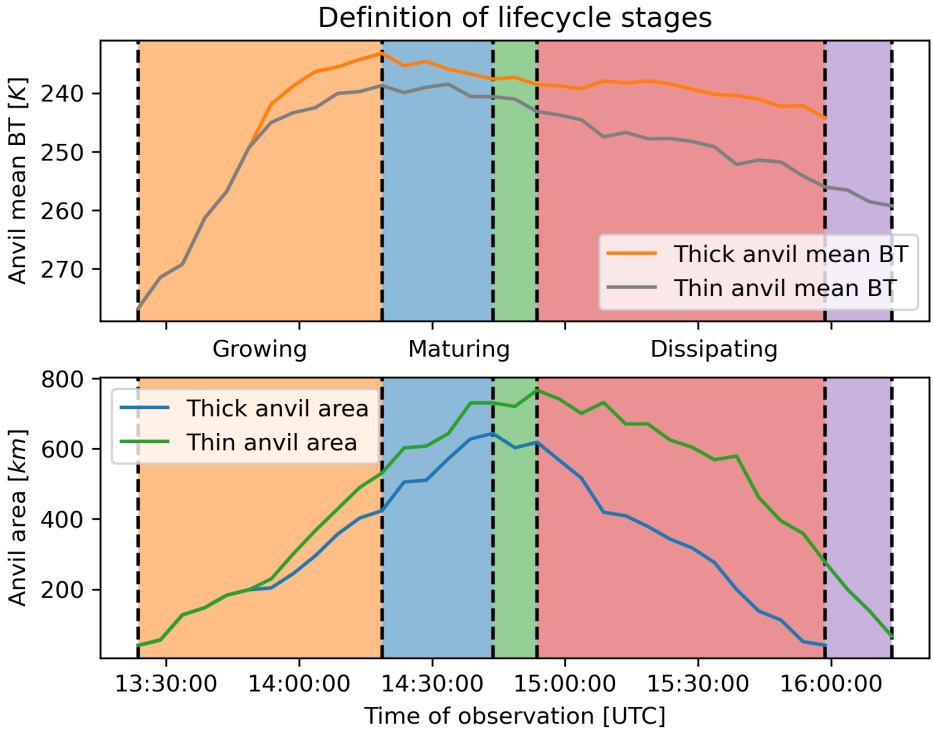

Figure 2. Definition of anvil lifecycle stages based on the method of Futyan and Del Genio (2007). The top panel shows the evolution of the mean BT of the thick and thin anvil regions over the DCC lifecycle, and the bottom panel shows the evolution of the anvil area. The growing phase (orange) is defined as the time between initial detection and the minimum observed BT. The mature phase for the thick (blue) and thin (green) anvil is defined as the time between the minimum BT and maximum thick and thin anvil area respectively. The dissipating phase for the thick (red) and thin (purple) anvils is defined as the time between the anvil maximum area and the final time of detection of the thick and thin anvil respectively.

We extend Futyan and Del Genio's method in this chapter through consideration of the development of both thick and thin anvil, which results in the lifecycle stages shown in fig. 2. The growing stage (orange) is defined as the time from the initial detection of the DCC to the time at which the thick anvil has its coldest average BT. The thick anvil maturation stage (blue) occurs between this time and the time at which the thick anvil reaches its maximum area, and the thin anvil maturing stage (green) occurs until the thin anvil reaches its maximum area. In this stage, the thin anvil continues to expand while the thick anvil begins to shrink. The thick anvil dissipating stage (red) ends at the final detection time of the thick anvil, while the thin anvil dissipating stage (purple) ends at the final detection time of the thin anvil, which is also the final detection time of the tracked DCC. By increasing the granularity of the lifecycle definition in this manner we can investigate how the impact of convective processes on DCC lifecycle might also impact their structure.

https://doi.org/10.5194/egusphere-2025-6391
Preprint. Discussion started: 30 December 2025

3.4 Composite analysis

To compare how the structure of tracked DCC evolve over their lifecycle, we interpolate the area of their cores, thick and thin anvils over a normalised lifetime. In this normalised lifetime, 0 is defined as the time of initial core detection, and 1 is the time of the final anvil detection. By normalising their lifetimes in this manner, the change over time of DCCs with different lifetimes can be composited and compared.

An example composite of the average properties of all analysed anvils in this chapter is shown in fig. 3. Figure 3 a shows the average change in area of the core (red), thick anvil (orange) and thin anvil (blue) over the normalised lifetime of the DCCs. Figure 3 b shows how these areas change as a proportion of the net DCC area. From fig. 3 b we can see how, on average, the structure of DCCs evolves over their lifetime. Initially, the DCC consists entirely of a growing core, with the maximum core area and the initial anvil formation occurring between 5% and 10% of the DCC lifetime. Between 10% and 40% of the normalised lifetime, while the anvil is maturing, the majority of the DCC consists of thick anvil, and the fraction of thin anvil increases slowly due to the similar rates of expansion of the thick and thin anvil. Beyond this point, the thick anvil reaches its maximum area before the thin anvil and dissipates faster, and the fraction of thin anvil increases until the end of the DCC lifecycle. Note that the average thin anvil fraction does not reach 100% at the end of the normalised lifetime due to the presence of some DCCs where we detect the dissipation of the thick and thin anvil to occur at the same time.

Through the use of composite analysis, we can investigate how the anvil structure changes throughout the DCC lifecycle in response to convective processes, rather than limiting our analysis to bulk properties or snapshots.

4 Results

4.1 Change in thin anvil fraction with intensity and organisation

To begin, we compare how the net thin anvil fraction of observed anvils changes with the mean anvil BT, initial core maximum cooling rate and number of cores. In fig. 4 a we show how the thin anvil proportion changes with the average thick anvil BT. Note that we only consider the thick anvil BT to avoid a dependence between the anvil BT and the thin anvil area. We see an increase of thin anvil proportion with the average anvil BT, agreeing with the results of Protopapadaki et al. (2017). Figure 4 b compares how the thin anvil fraction changes with the maximum cooling rate of the initial core associated with the anvil, and again shows a positive relation between the strength of convection and the thin anvil fraction. The measured proportion of thin anvil differs from that observed in previous studies, which is expected as different methods and thresholds are used to define thick and thin, and in this study the proportion is measured over the entire DCC lifetime rather than at a single point in time. Instead, it is the relative change of thin anvil fraction with changes in convective properties that is of importance.

In fig. 4 c, we compare the thin anvil fraction to the number of cores associated with each anvil. In contrast to fig. 4 a and b, no change is seen in the thin anvil fraction with an increase in the number of cores. As this occurs despite the tendency for multiple-core anvils to have colder average BT, this indicates that further factors are involved in changes in the thin anvil fraction than the temperature and height of the anvil.

https://doi.org/10.5194/egusphere-2025-6391
Preprint. Discussion started: 30 December 2025

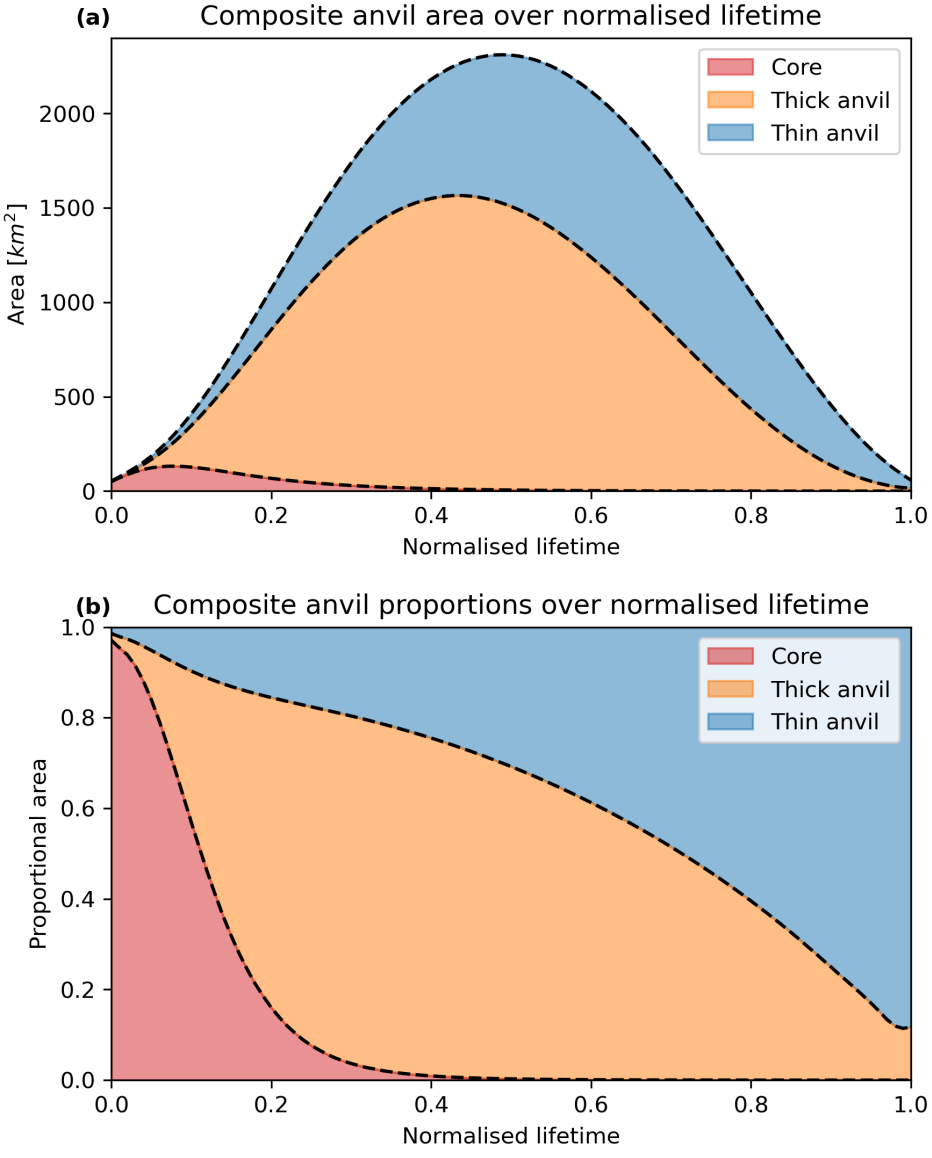

Figure 3. The average evolution of composites of cores (red), thick anvils (orange) and thin anvils (blue) over their normalised lifetimes, where 0 is the initial core detection time and 1 is the final anvil detection time. Panel (a) shows the average area of anvils, and (b) shows the proportion of the total area corresponding to each part of the anvil structure.

https://doi.org/10.5194/egusphere-2025-6391
Preprint. Discussion started: 30 December 2025

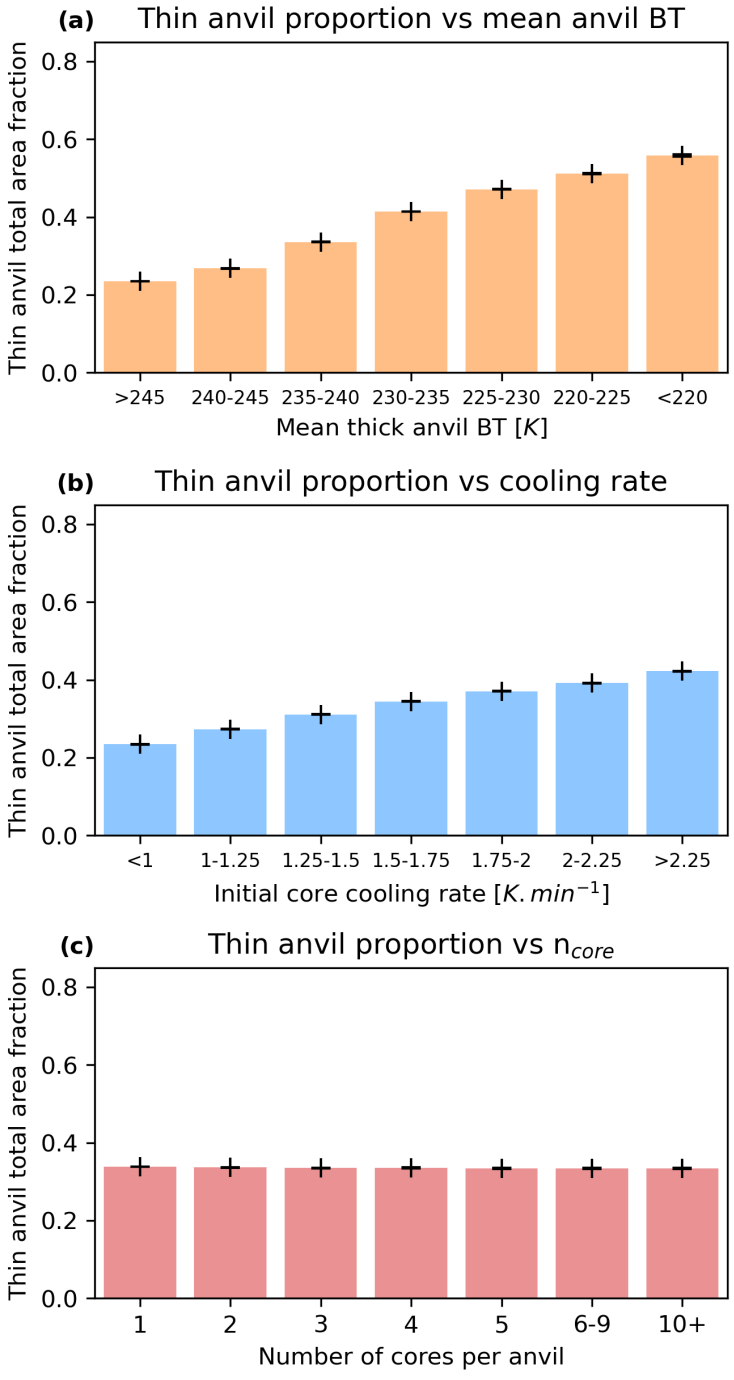

Figure 4. Thin anvil proportion of anvils categorised by (a) mean anvil BT, (b) initial core cooling rate, and (c) number of cores. Error bars show the standard error on the mean, and are too small to visualise in most cases.

https://doi.org/10.5194/egusphere-2025-6391
Preprint. Discussion started: 30 December 2025

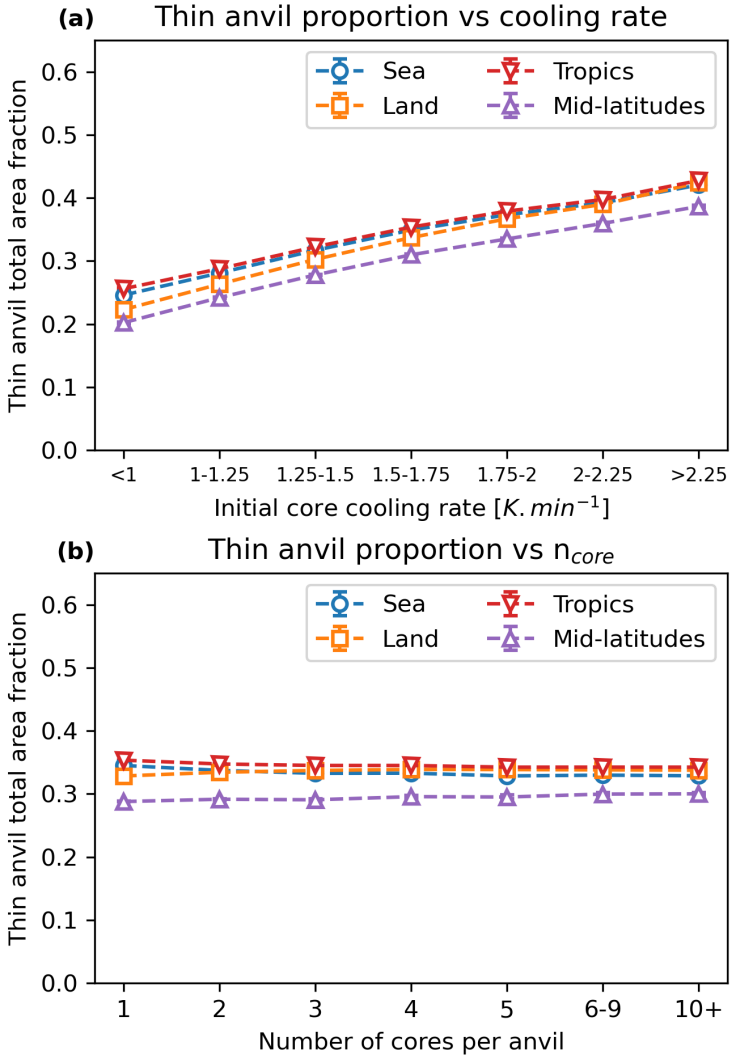

Figure 5. A comparison of the change in thin anvil proportion with (a) maximum core cooling rate and (b) number of cores for four different regions: sea (blue diamond markers), land (orange square markers), tropics (<30 °N; red downward triangle markers) and mid-latitudes (>30 °N; purple upward triangle markers). Error bars show the standard error on the mean, and are too small to visualise in most cases.

https://doi.org/10.5194/egusphere-2025-6391
Preprint. Discussion started: 30 December 2025

To ensure that these relationships are not caused by differences in the properties and distributions of DCCs across different regions, we further break down the relationship between cooling rate and number of cores and the thin anvil fraction with four different regions, shown in fig. 5. As with previous studies we find that the fraction of thin anvil is very similar for DCCs observed over land and ocean. While we do see a difference in the thin anvil fraction of approximately 0.05 between DCCs located in the tropics and mid-latitudes (defined as <30 °N and >30 °N respectively), this difference decreases slightly with both increasing convective intensity and number of cores. Overall, the near identical relationship of thin anvil fraction to intensity and organisation across multiple regions indicates that this is linked to the convective processes themselves, rather than a co-variance with local conditions.

4.2 Impact of intensity and organisation on DCC properties

Both the intensity and organisation of DCC cores have impacts on the properties of their anvil clouds. In this section we will investigate how these processes affect the bulk properties of these anvils; the anvil maximum area and the anvil lifetime for both thick and thin anvils, and the anvil BT. Comparing the bulk properties of these anvils provides an indication of how their structure changes, however, as we will see, they do not fully explain the differences shown in figs. 4 and 5.

In fig. 6 we show how the area, lifetime and BT of DCCs changes with the core cooling rate (right column) and number of cores (left column). Figure 6 a shows that the average thick and thin anvil maximum areas vary very little with cooling rate, except for at the highest observed values of cooling rate. There is however a slight widening in the gap between thick and thin anvil maximum area with increasing core cooling rate, as the thin anvil increases in maximum area while the thick anvil remains consistent. Both the thick and thin anvil maximum area increase substantially with an increasing number of cores (fig. 6 b). Figure 6 c shows that while the average thick anvil lifetime remains constant with increasing core cooling rate, the thin anvil lifetime increases. For increasing number of cores, there is an increase in both the thick and thin anvil lifetime with increasing number of cores shown in fig. 6 d. We also see a consistent decrease in both average and minimum thick anvil BT with cooling rate, shown in fig. 6 e, agreeing with the general usage of BT as a proxy for intensity. Similarly, there is a decrease of average anvil BT with the number of cores in fig. 6 f. The minimum anvil BT decreases at a notably faster rate with the increasing number of cores, however. Although this is indicative of an increased likelihood of overshooting cores in more organised DCCs, we must also note that the larger area of these systems also makes it more likely to observe colder pixels.

The changes in anvil properties with intensity and convection are intriguing due to both their differences and similarities. Both processes result in anvils with colder BT, which is commonly used as a proxy for convective intensity. However, the differences in the changes in anvil areas and lifetimes show that these processes cannot be lumped together so simply. In particular, the impact of intensity on the thin anvil properties without changing the bulk properties of the thick anvil show a clear impact of this process on anvil structure.

In fig. 7 we investigate how much of the thin anvil fraction can be attributed to the bulk changes in anvil maximum area and lifetime. We see that the proportional difference in the maximum area of the thick and thin anvils represents the majority of the change in thin anvil fraction across both convective intensity and organisation. This shows that while the trend in thin anvil fraction can be captured by snapshot observations from polar-orbiting satellites, they will underestimate the total changes

https://doi.org/10.5194/egusphere-2025-6391
Preprint. Discussion started: 30 December 2025

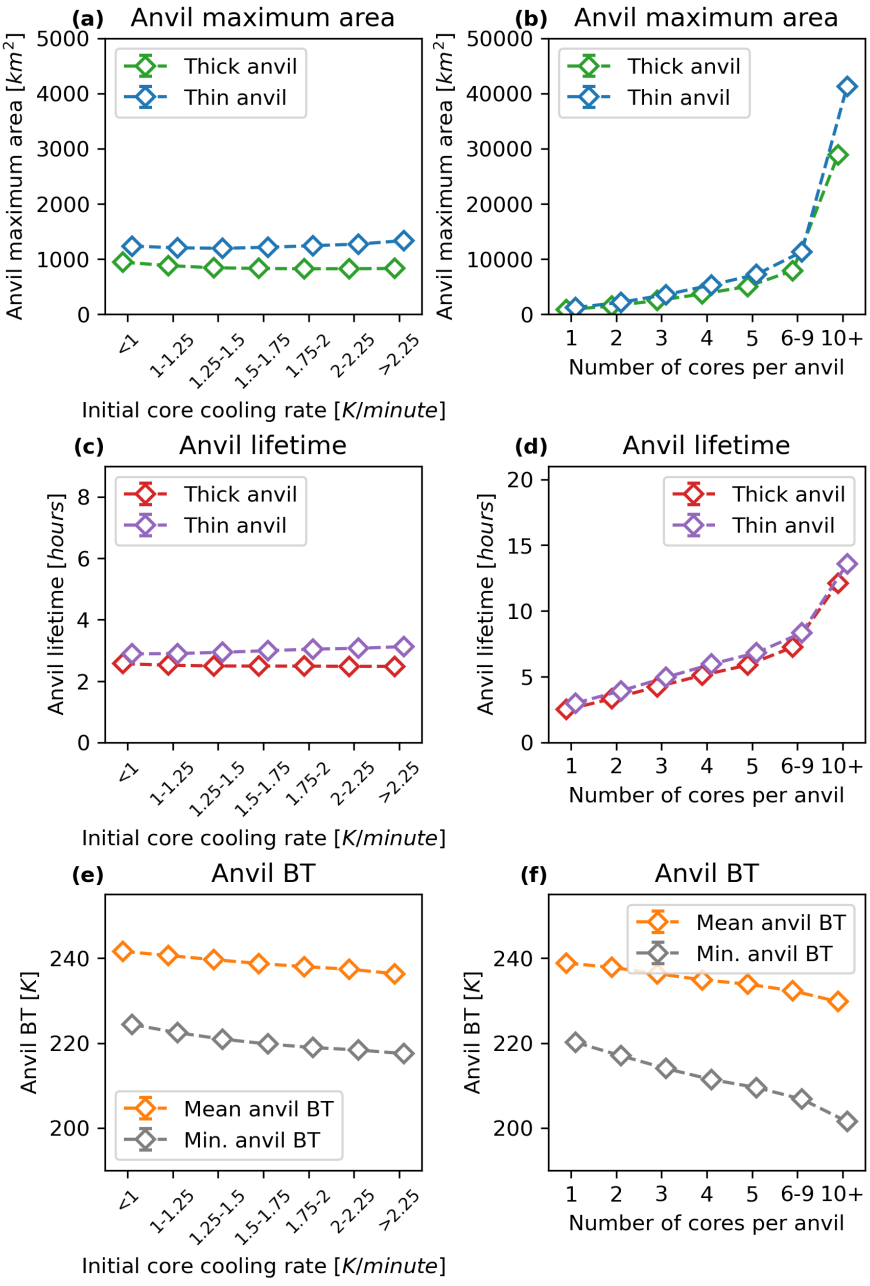

Figure 6. The changes in anvil area, lifetime, and mean and minimum BT observed for different core cooling rates and number of cores. Subfigures show changes in thick and thin anvil area (a, b), thick and thin anvil lifetime (c, d) and mean and minimum thick anvil BT (e, f). Plots on the left and right show changes with different core cooling rates and number of cores respectively. Error bars show the standard error on the mean, and are too small to visualise in most cases. Points have been staggered to show the thick and thin anvil properties more clearly, but correspond to the same tick marks on the x axis.

https://doi.org/10.5194/egusphere-2025-6391
Preprint. Discussion started: 30 December 2025

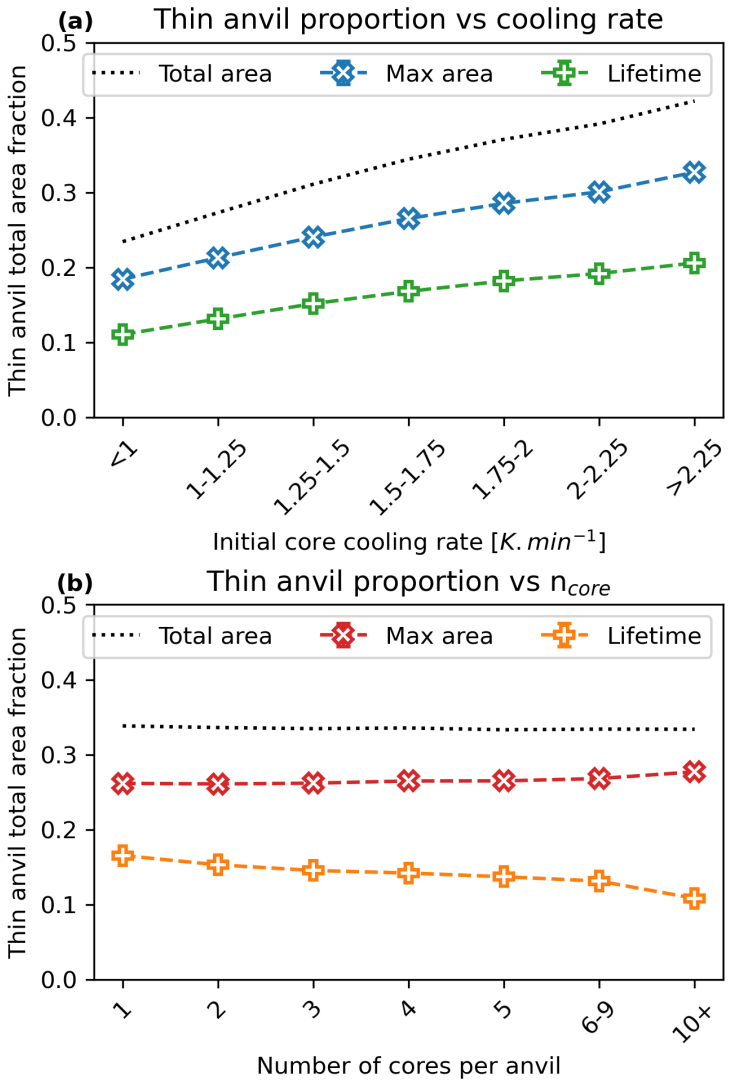

Figure 7. A comparison of the proportion of thin anvil measured at the time of maximum anvil area, and the proportional difference in lifetime, compared to the overall thin anvil proportion. Panel (a) shows the change in thin anvil proportion with core cooling rate, and (b) shows the changes with the number of cores. In both panels, the black dotted line shows the total thin anvil proportion over the entire DCC lifecycle. Error bars show the standard error on the mean, and are too small to visualise in most cases.

https://doi.org/10.5194/egusphere-2025-6391
Preprint. Discussion started: 30 December 2025

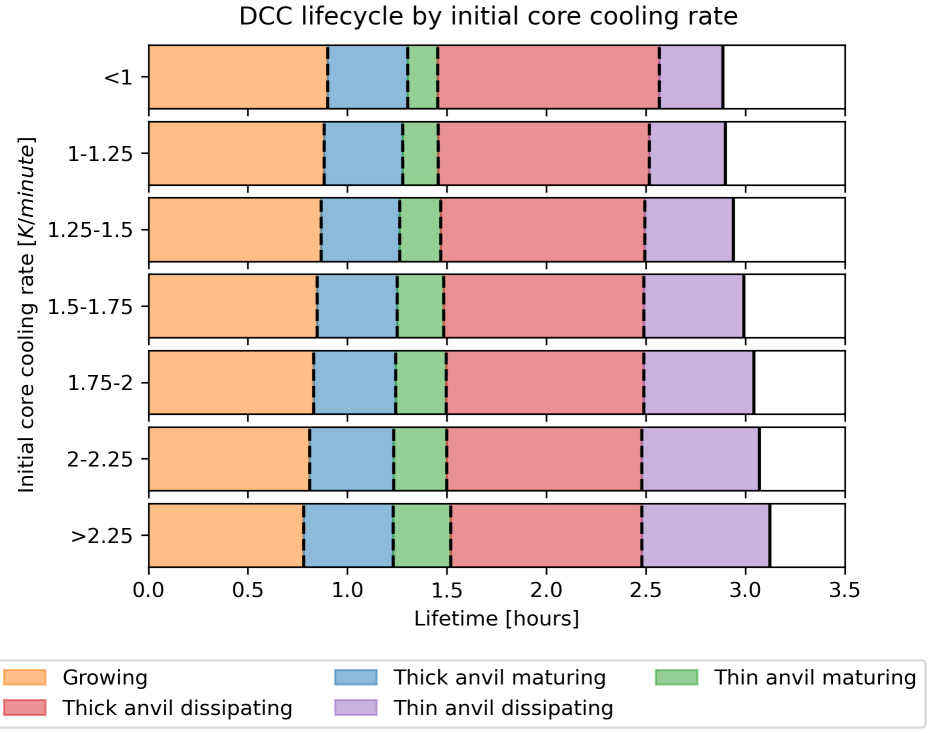

Figure 8. The lifetime of each of the lifecycle stages defined in section 3.3 for anvils categorised by initial core cooling rate.

in thin anvil fraction over the entire DCC lifetime. The proportional difference in the thick and thin anvil lifetimes shows a smaller contribution to the net thin anvil fraction. Furthermore, there is a stronger (positive) trend of the lifetime proportion with intensity and a weaker (negative) trend with organisation. For more organised DCCs, while the total average thin anvil fraction remains the same, the difference in the area of the thick and thin anvil increases but the difference in lifetime decreases, with these two changes cancelling each other.

4.3 Changes in DCC lifecycle with intensity and organisation

It is clear from the impact on anvil lifetime that both the intensity and organisation of convection affect DCC lifecycle. Furthermore, from fig. 7, we see that these different processes have different impacts on the lifecycle that warrant further investigation. In this section, we show how both convective processes affect the different lifecycle stages of DCCs. We use the modified Futyan and Del Genio method explained in section 3.3 throughout to break the anvil lifecycle into growing, mature and dissipating stages.

Figure 8 shows the lifetime of the different lifecycle stages for DCCs with increasing core cooling rates. The lifetime of the growing stage decreases from 55 to 45 minutes for the most intense convection. While these growing lifetimes are longer than those of the detected cores shown in Jones and Stier (2025), the trend agrees with the shorter lifetime for more intense cores.

https://doi.org/10.5194/egusphere-2025-6391
Preprint. Discussion started: 30 December 2025

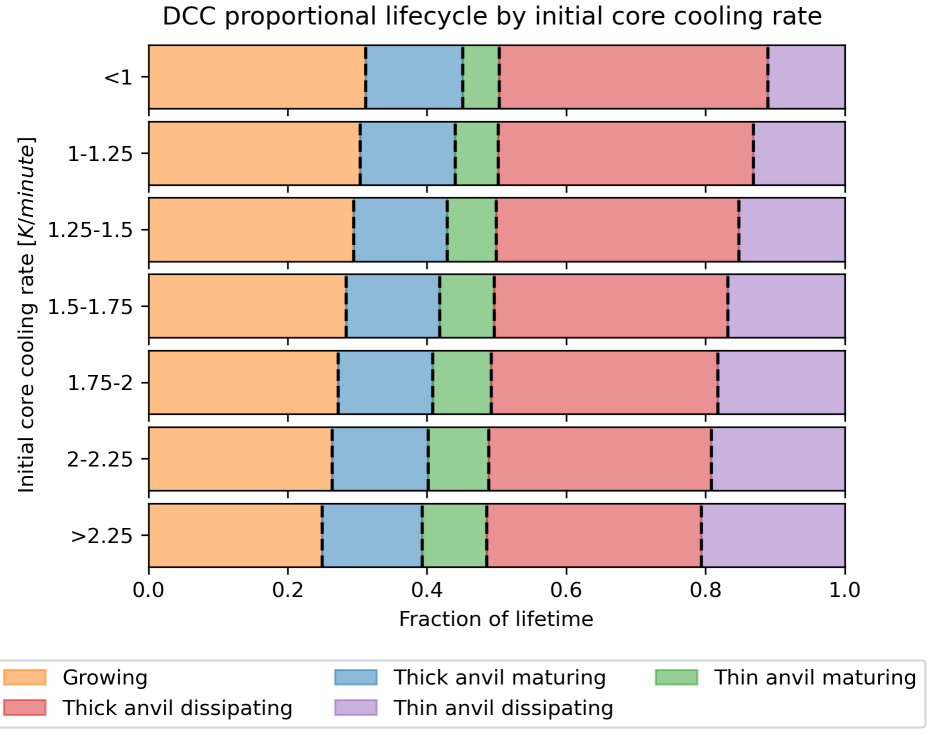

Figure 9. The average fraction of anvil lifetime of each of the lifecycle stages defined in section 3.3 for anvils categorised by initial core cooling rate. Each bar is normalised such that the total length of the row is equal to the mean thin anvil lifetime of its cooling rate bin.

Despite the colder BT and hence higher cloud top heights exhibited by these DCCs, the stronger vertical growth rates result in an anvil which reaches its minimum BT in a shorter time frame.

The timing of the maximum extent of the thick anvil is around 1.25 hours, and decreases slightly with increasing cooling rate, while the time of the maximum thin anvil area increases slightly for the most intense DCCs. Similarly, the timing of the dissipation of the thick remains mostly consistent at just over 2.5 hours for most cooling rates, however the thin anvil dissipation time increases below to avove 3 hours for more intense DCCs. These findings reinforce what was shown in fig. 6 c: that the core cooling rate affects the lifetime of the thin anvil much more than the thick anvil.

Figure 9 displays the average proportion of anvil lifetime spent in each of the stages shown in fig. 8. We normalise the anvil lifetime using the method described in section 3.4, where 0 is the time of the initial detection of the DCC and 1 is the time of the final detection of the dissipating thin anvil. By analysing these lifecycle stages as a proportion of the total lifetime, we can gain better insight into how changes in lifecycle impact the structure and bulk properties of observed DCCs.

The reduction in the lifetime of the growing phase and increase for thin anvil dissipation for more intense DCCs is again apparent. The time between these two stages, representing the period in which the thick anvil matures and then dissipates, lasts for around 60% of the total anvil lifecycle for all core cooling rates. The shorter growing period and longer thin anvil

https://doi.org/10.5194/egusphere-2025-6391
Preprint. Discussion started: 30 December 2025

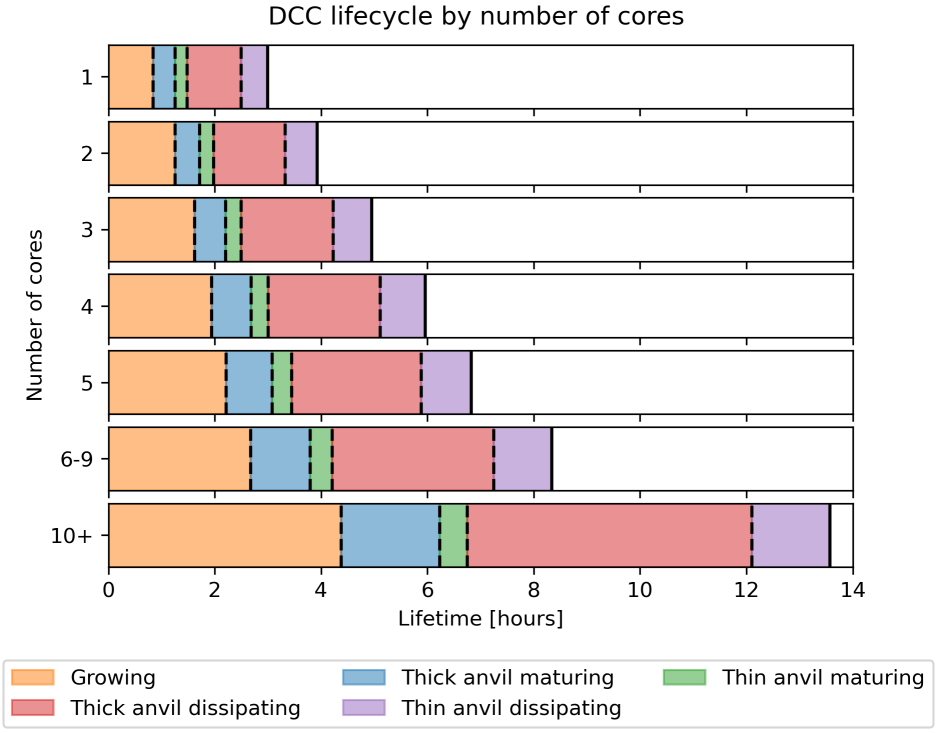

Figure 10. The average lifetime of each of the lifecycle stages defined in section 3.3 for anvils categorised by number of cores.

dissipating period act together to shift the evolution of the thick anvil earlier in the DCC lifecycle for more intense DCCs. For DCCs over land, where there is a pronounced peak in occurrence in the afternoon, we expect this to shift the time in which the anvil is at its thickest and has the largest extent earlier in the day, with potential impacts on its SW cloud radiative effect (CRE).

Figure 10 shows how the timing of the different anvil stages changes with increasing number of cores. It is immediately apparent that the large increase in overall lifetime with number of cores shown in fig. 6 d also applies to each of the lifecycle stages. This increase in lifetime occurs to such an extent that the average growing period for DCCs with 10 or more cores lasts longer than the average of the entire lifetime of isolated DCCs. The large spread in lifetimes makes it difficult to compare how the lifecycle changes with organisation, and so we move immediately to the normalised lifetime view.

Figure 11 shows the lifetime of each lifecycle stage as a proportion of the total lifetime for DCCs with different numbers of cores, in the same manner as used for fig. 9. In contrast to the effect of increasing intensity, we see that with increasing organisation the length of the growing phase increases and the length of the thin anvil dissipating phase decreases as a proportion of the overall lifetime. We see a similar behaviour of the period from the start of the mature phase to the thick anvil dissipation, which remains a consistent length for all core counts. With increasing organisation this period shifts later in the lifetime of the DCC.

https://doi.org/10.5194/egusphere-2025-6391
Preprint. Discussion started: 30 December 2025

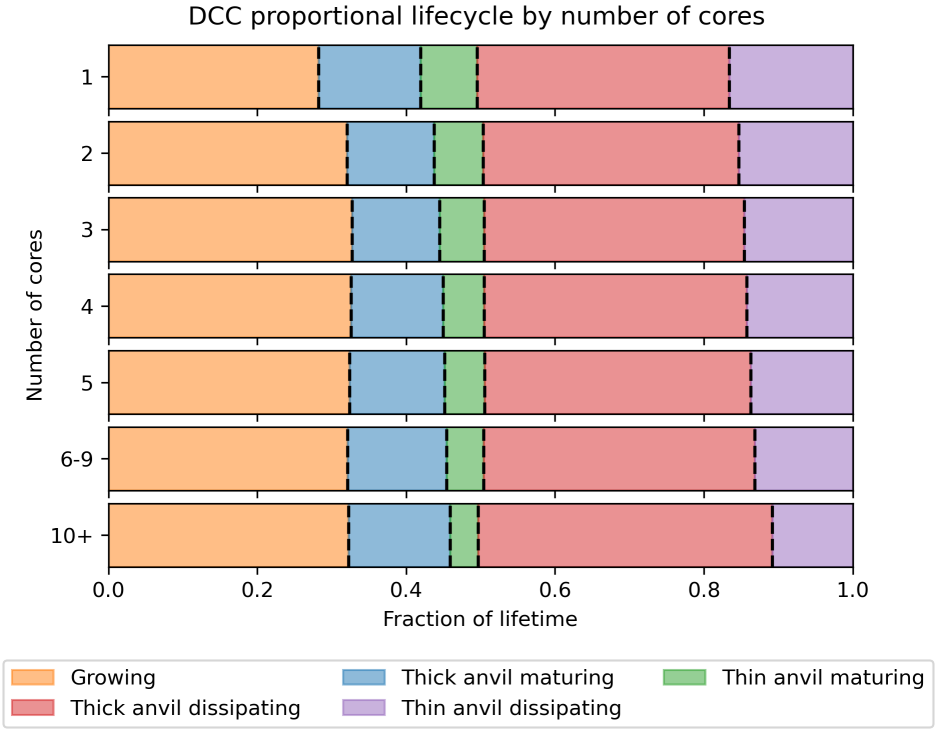

Figure 11. The average fraction of anvil lifetime of each of the lifecycle stages defined in section 3.3 for anvils categorised by number of cores. Each bar is normalised such that the total length of the row is equal to the mean thin anvil lifetime of its number of cores bin.

It should be clarified, however, that these differences are only in relation to the proportion of total lifetime. While more organised systems spend a smaller proportion of their lifetime in the thin anvil dissipating phase, the much greater overall lifetime means that this stage still lasts substantially longer than for DCCs with fewer cores.

4.4 Changes in thin anvil fraction over DCC lifecycle

While the contrasting changes in DCC lifecycle with increasing intensity and organisation (in particular the change in the thin anvil dissipating stage) go some way to explaining the difference in the thin anvil fraction, we have already seen in fig. 7 that the change in lifetime cannot account for the change in thin anvil fraction alone. The contrasting changes in lifecycle do, however, indicate that the two convective processes influence how DCCs evolve over their entire lifetimes. To further investigate how convective processes impact structure and lifecycle, we use the composite area approach described in section 3.4 to show how the thin anvil fraction evolves over the anvil lifecycle for DCCs with differing core cooling rates and number of cores.

Figure 12 shows composites of the thin anvil fraction for DCCs group by core cooling rate, with larger cooling rates shown in darker shades of blue. Each of the composites has a similar shape to the evolution of thin anvil fraction shown in fig. 3 b; an initial increase as the anvil develops, a slower period of thin anvil fraction growth during the maturing stage, and a continual

https://doi.org/10.5194/egusphere-2025-6391
Preprint. Discussion started: 30 December 2025

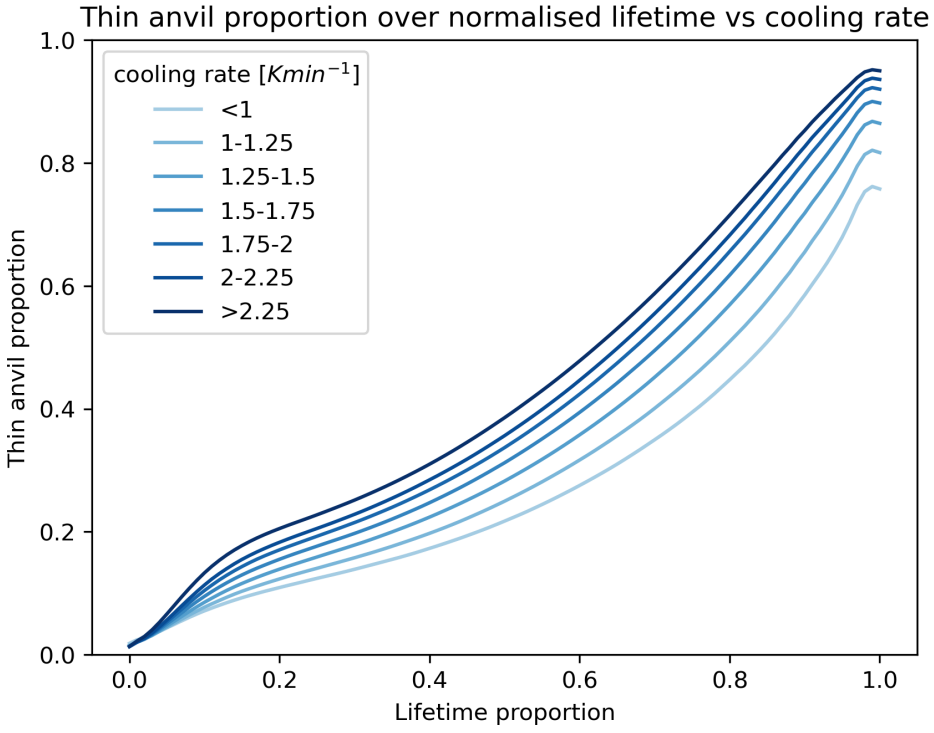

Figure 12. Mean thin anvil proportion for composites of anvil area of normalised lifetime categorised by the cooling rate of their initial cores. More intense core cooling rates are shown by the darker blue lines.

increase in the rate of thin anvil fraction as the anvil dissipates. Two sections of the lifecycle show divergence in the thin anvil fraction with core cooling rate. Firstly, more intense cores produce a higher thin anvil fraction during the developing phase when the anvil initially forms. This difference in thin anvil fraction is then maintained throughout the mature phase. Secondly, the thin anvil fraction further diverges during the dissipating phase, with the anvils originating from more intense cores having a larger increase in thin anvil fraction. This difference during the dissipating stage may be related to the difference in the thin anvil lifetime seen previously.

In fig. 13 we compare how the mean thin anvil fraction changes for composites grouped by the number of cores. The composites with a greater number of cores are shown by the darker shades of red. In contrast to fig. 12, we see a difference from the typical shape of the thin anvil fraction established in fig. 3 for more organised DCCs. At the end of the initial development phase of the anvil we see a similar thin anvil fraction of $\tilde{0}.2$ across all cases. While the more organised DCCs reach this point faster, this is simply due to the initial anvil formation time making up a smaller proportion of the total lifetime due to the increase in the overall anvil lifetime with organisation.

https://doi.org/10.5194/egusphere-2025-6391
Preprint. Discussion started: 30 December 2025

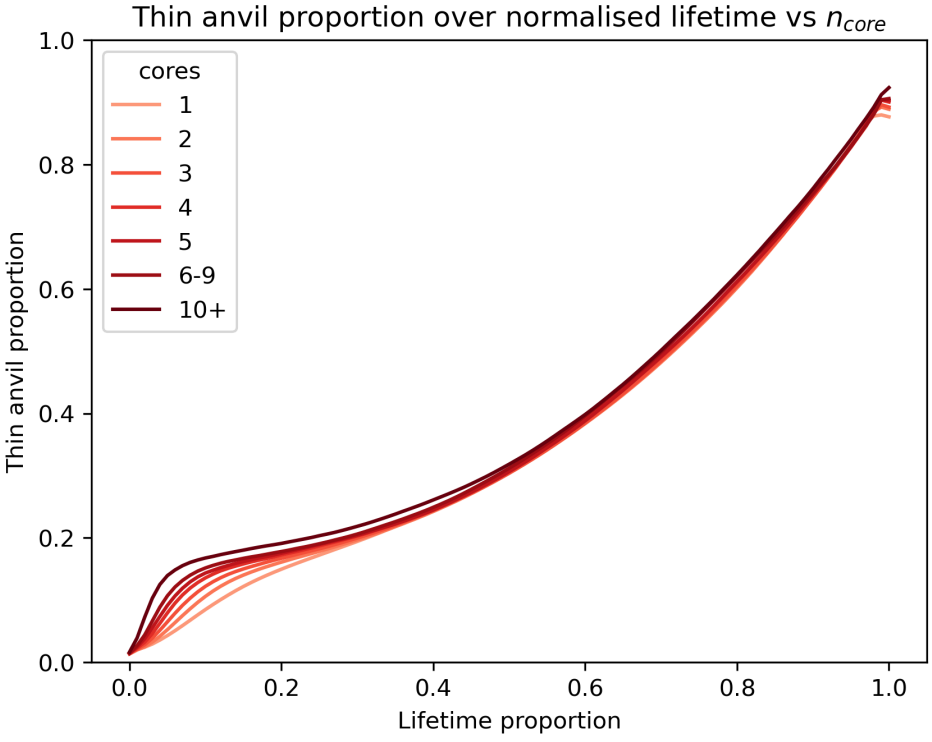

Figure 13. Mean thin anvil proportion for composites of anvil area of normalised lifetime categorised by the number of cores. Anvils with a larger number of cores are shown by the darker red lines.

After the initial development of the anvil, unlike for DCCs with different intensities, very little difference is seen in the thin anvil fraction and its evolution across the mature and dissipating stages for DCCs with different numbers of cores, despite the large difference in the anvil area and lifetime. This similarity in the development of the anvil cloud agrees with previous results which found characteristic growth and decay rates for anvil clouds across a wide range of sizes using cloud tracking (Roca et al., 2017).

The investigation of changes in thin anvil fraction over DCC lifecycle using composites reveals further complexity to the response of thin anvil structure to convective processes. Not only do changes in intensity and organisation have different effects on the net thin anvil fraction and the lifecycle, they also impact the anvil structure at different stages throughout the DCC lifetime. The timing of when then differences in structure occur may help in investigating the processes which cause these changes.

https://doi.org/10.5194/egusphere-2025-6391
Preprint. Discussion started: 30 December 2025

5 Conclusions

Deep convective anvil clouds have a characteristic ToA CRE that is near neutral (Hartmann, 2016). Anvils are, however, not homogeneous objects, and exhibit structures that transition from thick near the convective cores to thin, detrained cirrus further away. The tendency of reflectivity to reduce faster than emissivity with reducing cloud optical thickness, combined with the large SW and LW CRE of anvils, means that the CRE varies widely with changing thickness (Berry and Mace, 2014). Despite this, the response of anvil optical properties to climate change remains largely uncertain, in part due to the lack of data connecting the behaviour of convective cores and anvils Gasparini et al. (2023).

Previous studies have found that the fraction of thin anvil increases with increasing convective intensity (Protopapadaki et al., 2017; Takahashi et al., 2017). These studies were performed using sun-synchronous polar-orbiting satellite data, and so could not resolve changes across the lifecycle of DCCs. Using a dataset of tracked DCC cores and anvils we can relate changes in the convective properties to changes in structure observed over the entire anvil lifecycle.

Using the initial core cooling rate and number of cores as proxies for the intensity and organisation of convection respectively, we find a similar increase in thin anvil fraction with increasing intensity, but no change with increasing organisation. The relationships are found to be robust across a wide range of convective environments. We also find contrasting impacts on DCC lifecycle as a result of both processes. In more intense DCCs, we see a reduction in the growing phase and an increase in the thin anvil lifetime, whereas we see the opposite in more organised cases. These corresponding changes in lifecycle indicate that the thin anvil fraction cannot be fully determined from single snapshots alone.

By analysing composites of the change in thin anvil fraction over the DCC lifecycle, we see that the impacts of intensity and organisation also occur at different periods during the DCC lifetime. The timing of these changes also indicates which processes may be impacting the anvil structure in each case. For the more intense convection, we see an increase in the thin anvil fraction during the initial formation of the anvil, which is then maintained as the anvil matures. Studies of anvil evolution in high-resolution convective resolving models have shown that, during the initial growth of the anvil, before the development of compensating downdrafts within the core, the divergence of the anvil is directly linked to the updraft velocities within the core (Senf et al., 2018). After the formation of compensating downdrafts after around 15–20 minutes, this connection is broken which may explain why this difference only occurs during the very early formation of the anvil.

We also see a second period of increasing difference in thin anvil fraction during the dissipating stage of the DCCs. As this occurs after the end of the convective updrafts, it cannot be related directly to the convective processes but instead to their impact on the anvil properties. Over the lifetime of anvils, radiative heating of the cloud base and cooling of the cloud top result in circulations within the anvil cloud which have a thinning effect (Gasparini et al., 2019). Once the anvil is sufficiently thin however (with optical depths around 1), these radiatively driven circulations cease and instead the remainder of the dissipation occurs due to the sedimentation and sublimation of the remaining thin cirrus (Sokol and Hartmann, 2020). At the higher altitudes and colder temperatures of the anvils produced by more intense convection these processes are substantially slower (Seeley et al., 2019), potentially resulting in larger extents and lifetimes for the thin, but not thick, anvil.

https://doi.org/10.5194/egusphere-2025-6391
Preprint. Discussion started: 30 December 2025

For more organised DCCs we observe a difference in the intitial anvil formation, but consistently similar thin anvil fraction throughout the mature and dissipating stages of the anvil lifecycle, despite the large differences in the average area, lifetime and temperature of DCCs with different number of cores. The convergence of the thin anvil fraction during the dissipating phase of DCCs is indicative of the characteristic decay patterns seen in convective anvils across scales (Roca et al., 2017; Elsaesser et al., 2022).

Care should be taken when interpreting these results to consider covariance in the metrics used to measure convective intensity and organisation with the measured anvil structure. In particular, the occurrence of thicker anvil clouds may result in the detection algorithm considering two neighbouring DCCs as forming a single cloud shield, when otherwise they would be considered isolated. This may result in a confounding factor where the anvil structure is affecting the number of cores, rather than the other way around. Further analysis into the observations of organised convection and their dynamics could reveal more about the processes affecting the structure of these clouds, as well as examine differences in different modes of organised convection (such as tropical cloud clusters vs linear squall lines) which may show different behaviours regarding their structure.

A limitation of the simple separation of thick and thin anvil is that uniform changes in anvil thickness cannot be distinguished from changes in the anvil thickness distribution. An anvil that is uniformly thicker will result in a larger thick anvil area and a smaller thin anvil fraction. For a straightforward analysis of the impact of changes in anvil structure on the climate this is not a significant difference, as anvil CRE is most sensitive to changes in thickness at OD around 2 (Berry and Mace, 2014), and so the cutoff value for thick anvil is ideal. More detailed analysis of the mechanisms through which anvil structure changes may, however, require more information about the overall distribution of anvil thickness that is not provided by these metrics. Use of retrieved cloud properties, or colocation with cloud radar instruments that can resolve the vertical structure of anvil clouds (such as in Elsaesser et al. (2022)) , may be important for further understanding of processes affecting anvil thickness.

However, further investigation of how these processes impact anvil structure and lifecycle from observations may be difficult due to the lack of time-resolved data that can measure these processes. The use of modelling, including both convective resolving models and more idealised experiments, may provide a route to isolate the impacts of each process on DCC evolution (Gasparini et al., 2022). Lifecycle analysis provides opportunities for new constraints on the representation of DCCs in convective resolving models. Analysis of km-scale models has revealed responses of anvil structure to changes in convection (Sokol et al., 2024), however as this was performed using bulk analysis it does not provide any insight into the processes which cause this response, or why models differ from each other. Although geostationary satellite observations cannot observe these processes directly, studying the behaviour of DCCs over time may provide insight into the relative impacts on different processes. For example, in fig. 12, changes in the anvil structure are seen at two points during the convective lifecycle. Changes to the anvil during its initial formation can be linked to the convective dynamics themselves, whereas those during the dissipating phase may instead be a result of in situ anvil processes as by this point in the lifecycle the convective dynamics have stopped. Comparing how anvils in convective resolving models evolve over time to observations may help identify which processes are important to anvil structure and their relative influence, even if these processes cannot be observed themselves.

https://doi.org/10.5194/egusphere-2025-6391
Preprint. Discussion started: 30 December 2025

The final element to consider is how these observed changes in anvil structure may impact the anvil CRE. Pilewskie and L'Ecuyer (2025) found that more intense convection is linked to more warming anvil CRE due to both the thinner structure and the colder temperature of the anvil clouds. While changes in organisation also affect the anvil cloud temperature, the results found here suggest that they would not have as strong a warming effect overall due to the lack of structural changes. Furthermore, the observed changes in the lifecycle and the timing of the maximum extent of the thick anvil within the DCC lifetime may impact the SW CRE, particularly over land due to the pronounced diurnal cycle of convection. Observational studies have, shown a link between increasing convective organisation and domain mean ToA cooling (Bony et al., 2020). While this has traditionally been explained as a result of greater clear sky LW emissions to space (Bony et al., 2016), this could also result from the response of anvil CRE to changes in structure. With the latest studies anvil thinning in response to warming (e.g. Raghuraman et al., 2024; Sokol et al., 2024), along with evidence of changes to convective intensity, organisation and the net convective overturning circulation (e.g. Seeley and Romps, 2015; Bao et al., 2024; Williams and Jeevanjee, 2025), it is vital that we understand the mechanisms through which changes in convective processes affect anvil CRE for climate feedbacks.

Code and data availability. The dataset from Jones and Stier (2025) used in this article is publicly archived on zenodo: (Jones, 2025b). The jupyter notebooks used for data analysis and the generation of the plots shown in this article, along with all other material used to prepare the article, are publicly archived on zenodo: (Jones, 2025a). The GOES-16 ABI data used in this study is available from NOAA and is archived on Amazon Web Services, Google Cloud, and NOAA CLASS: (GOES-R Algorithm Working Group and GOES-R Series Program, 2017)

Author contributions. WKJ designed the study, performed the data analysis and validation, and wrote this paper with contributions and feedback from PS.

Competing interests. At least one of the (co-)authors is a member of the editorial board of *Atmospheric Chemistry and Physics*

Acknowledgements. The authors acknowledge financial support from the European Research Council (ERC) Horizon programme grant nos. 724602 (RECAP), 821205 (FORCeS), 101003470 (NextGEMS) and 101137639 (CleanCloud). This work was performed on JASMIN, the UK collaborative data analysis facility, and LOTUS, the associated high performance batch compute cluster. GOES-16 ABI data provided by the NOAA open data dissemination (NODD) program. The authors would like to thank Sue van den Heever and Graeme Stephens for the discussions that led to the design of this study.

https://doi.org/10.5194/egusphere-2025-6391
Preprint. Discussion started: 30 December 2025

References

Augustine, J. A. and Howard, K. W.: Mesoscale Convective Complexes over the United States during 1985, Monthly Weather Review, 116, 685–701, https://doi.org/10.1175/1520-0493(1988)116<0685:MCCOTU>2.0.CO;2, 1988.

Bao, J., Stevens, B., Kluft, L., and Muller, C.: Intensification of Daily Tropical Precipitation Extremes from More Organized Convection, Science Advances, 10, eadj6801, https://doi.org/10.1126/sciadv.adj6801, 2024.

Berry, E. and Mace, G. G.: Cloud Properties and Radiative Effects of the Asian Summer Monsoon Derived from A-Train Data, Journal of Geophysical Research: Atmospheres, 119, 9492–9508, https://doi.org/10.1002/2014JD021458, 2014.

Bony, S., Stevens, B., Coppin, D., Becker, T., Reed, K. A., Voigt, A., and Medeiros, B.: Thermodynamic Control of Anvil Cloud Amount, Proceedings of the National Academy of Sciences, 113, 8927–8932, https://doi.org/10.1073/pnas.1601472113, 2016.

Bony, S., Semie, A., Kramer, R. J., Soden, B., Tompkins, A. M., and Emanuel, K. A.: Observed Modulation of the Tropical Radiation Budget by Deep Convective Organization and Lower-Tropospheric Stability, AGU Advances, 1, e2019AV000155, https://doi.org/10.1029/2019AV000155, 2020.

DeWitt, T. D. and Garrett, T. J.: Finite Domains Cause Bias in Measured and Modeled Distributions of Cloud Sizes, Atmospheric Chemistry and Physics, 24, 8457–8472, https://doi.org/10.5194/acp-24-8457-2024, 2024.

Elsaesser, G. S., Roca, R., Fiolleau, T., Del Genio, A. D., and Wu, J.: A Simple Model for Tropical Convective Cloud Shield Area Growth and Decay Rates Informed by Geostationary IR, GPM, and Aqua/AIRS Satellite Data, Journal of Geophysical Research: Atmospheres, 127, https://doi.org/10.1029/2021JD035599, 2022.

Emde, C., Buras-Schnell, R., Kylling, A., Mayer, B., Gasteiger, J., Hamann, U., Kylling, J., Richter, B., Pause, C., Dowling, T., and Bugliaro, L.: The libRadtran Software Package for Radiative Transfer Calculations (Version 2.0.1), Geoscientific Model Development, 9, 1647–1672, https://doi.org/10.5194/gmd-9-1647-2016, 2016.

Futyan, J. M. and Del Genio, A. D.: Deep Convective System Evolution over Africa and the Tropical Atlantic, Journal of Climate, 20, 5041–5060, https://doi.org/10.1175/JCLI4297.1, 2007.

Gasparini, B., Blossey, P. N., Hartmann, D. L., Lin, G., and Fan, J.: What Drives the Life Cycle of Tropical Anvil Clouds?, Journal of Advances in Modeling Earth Systems, 11, 2586–2605, https://doi.org/10.1029/2019MS001736, 2019.

Gasparini, B., Sokol, A. B., Wall, C. J., Hartmann, D. L., and Blossey, P. N.: Diurnal Differences in Tropical Maritime Anvil Cloud Evolution, Journal of Climate, 35, 1655–1677, https://doi.org/10.1175/JCLI-D-21-0211.1, 2022.

Gasparini, B., Sullivan, S. C., Sokol, A. B., Kärcher, B., Jensen, E., and Hartmann, D. L.: Opinion: Tropical Cirrus – from Micro-Scale Processes to Climate-Scale Impacts, Atmospheric Chemistry and Physics, 23, 15 413–15 444, https://doi.org/10.5194/acp-23-15413-2023, 2023.

GOES-R Algorithm Working Group and GOES-R Series Program: NOAA GOES-R Series Advanced Baseline Imager (ABI) Level 2 Cloud and Moisture Imagery Products (CMIP), https://doi.org/10.7289/V5736P36, 2017.

Hartmann, D. L.: Tropical Anvil Clouds and Climate Sensitivity, Proceedings of the National Academy of Sciences, 113, 8897–8899, https://doi.org/10.1073/pnas.1610455113, 2016.

Hartmann, D. L., Ockert-Bell, M. E., and Michelsen, M. L.: The Effect of Cloud Type on Earth's Energy Balance: Global Analysis, Journal of Climate, 5, 1281–1304, https://doi.org/10.1175/1520-0442(1992)005<1281:TEOCTO>2.0.CO;2, 1992.

https://doi.org/10.5194/egusphere-2025-6391
Preprint. Discussion started: 30 December 2025

Henderson, D. S., Otkin, J. A., and Mecikalski, J. R.: Evaluating Convective Initiation in High-Resolution Numerical Weather Prediction Models Using GOES-16 Infrared Brightness Temperatures, Monthly Weather Review, 149, 1153–1172, https://doi.org/10.1175/MWR-D-20-0272.1, 2021.

Horner, G. and Gryspeerdt, E.: The Evolution of Deep Convective Systems and Their Associated Cirrus Outflows, Atmospheric Chemistry and Physics, 23, 14 239–14 253, https://doi.org/10.5194/acp-23-14239-2023, 2023.

Jones, W.: Material for preparation of "Effects of convective intensity and organisation on the structure and lifecycle of deep convective clouds" [code], https://doi.org/10.5281/zenodo.17991287, 2025a.

Jones, W.: Tobac-Flow Tracked DCCs in GOES ABI CONUS Region 2018-2024 [dataset], https://doi.org/10.5281/zenodo.17296632, 2025b.

Jones, W. K. and Stier, P.: Linking the Properties of Deep Convective Cores and Their Associated Anvil Clouds Observed over North America, ESS Open Archive, https://doi.org/10.22541/essoar.176114366.69683239/v1, 2025.

Jones, W. K., Christensen, M. W., and Stier, P.: A Semi-Lagrangian Method for Detecting and Tracking Deep Convective Clouds in Geostationary Satellite Observations, Atmospheric Measurement Techniques, 16, 1043–1059, https://doi.org/10.5194/amt-16-1043-2023, 2023.

Lindzen, R. S., Chou, M.-D., and Hou, A. Y.: Does the Earth Have an Adaptive Infrared Iris?, Bulletin of the American Meteorological Society, 82, 417–432, https://doi.org/10.1175/1520-0477(2001)082<0417:DTEHAA>2.3.CO;2, 2001.

Luo, Z. and Rossow, W. B.: Characterizing Tropical Cirrus Life Cycle, Evolution, and Interaction with Upper-Tropospheric Water Vapor Using Lagrangian Trajectory Analysis of Satellite Observations, Journal of Climate, 17, 4541–4563, https://doi.org/10.1175/3222.1, 2004.

Maddox, R. A.: Mesoscale Convective Complexes, Bulletin of the American Meteorological Society, 61, 1374–1387, 1980.

Massie, S., Gettelman, A., Randel, W., and Baumgardner, D.: Distribution of Tropical Cirrus in Relation to Convection, Journal of Geophysical Research: Atmospheres, 107, AAC 19–1–AAC 19–16, https://doi.org/10.1029/2001JD001293, 2002.

McKim, B., Bony, S., and Dufresne, J.-L.: Weak Anvil Cloud Area Feedback Suggested by Physical and Observational Constraints, Nature Geoscience, pp. 1–6, https://doi.org/10.1038/s41561-024-01414-4, 2024.

Pilewskie, J. and L'Ecuyer, T.: The Role of Convective Intensity in Modulating the Earth's Radiative Balance, Journal of Climate, -1, https://doi.org/10.1175/JCLI-D-24-0334.1, 2025.

Protopapadaki, S. E., Stubenrauch, C. J., and Feofilov, A. G.: Upper Tropospheric Cloud Systems Derived from IR Sounders: Properties of Cirrus Anvils in the Tropics, Atmospheric Chemistry and Physics, 17, 3845–3859, https://doi.org/10.5194/acp-17-3845-2017, 2017.

Raghuraman, S. P., Medeiros, B., and Gettelman, A.: Observational Quantification of Tropical High Cloud Changes and Feedbacks, Journal of Geophysical Research: Atmospheres, 129, e2023JD039 364, https://doi.org/10.1029/2023JD039364, 2024.

Roberts, R. D. and Rutledge, S.: Nowcasting Storm Initiation and Growth Using GOES-8 and WSR-88D Data, Weather and Forecasting, 18, 562–584, https://doi.org/10.1175/1520-0434(2003)018<0562:NSIAGU>2.0.CO;2, 2003.

Roca, R., Fiolleau, T., and Bouniol, D.: A Simple Model of the Life Cycle of Mesoscale Convective Systems Cloud Shield in the Tropics, Journal of Climate, 30, 4283–4298, https://doi.org/10.1175/JCLI-D-16-0556.1, 2017.

Schmit, T. J., Griffith, P., Gunshor, M. M., Daniels, J. M., Goodman, S. J., and Lebair, W. J.: A Closer Look at the ABI on the GOES-R Series, Bulletin of the American Meteorological Society, 98, 681–698, https://doi.org/10.1175/BAMS-D-15-00230.1, 2016.

Schmit, T. J., Lindstrom, S. S., Gerth, J. J., and Gunshor, M. M.: Applications of the 16 Spectral Bands on the Advanced Baseline Imager (ABI)., Journal of Operational Meteorology, 06, 33–46, https://doi.org/10.15191/nwajom.2018.0604, 2018.

Seeley, J. T. and Romps, D. M.: Why Does Tropical Convective Available Potential Energy (CAPE) Increase with Warming?, Geophysical Research Letters, 42, 10,429–10,437, https://doi.org/10.1002/2015GL066199, 2015.

https://doi.org/10.5194/egusphere-2025-6391
Preprint. Discussion started: 30 December 2025

Seeley, J. T., Jeevanjee, N., Langhans, W., and Romps, D. M.: Formation of Tropical Anvil Clouds by Slow Evaporation, Geophysical Research Letters, 46, 492–501, https://doi.org/10.1029/2018GL080747, 2019.

Senf, F., Lenk, S., Deneke, H., and Heinze, R.: High-Resolution Simulations of Deep Convective Growth and Meteosat Observations, 2018.

Sherwood, S. C., Webb, M. J., Annan, J. D., Armour, K. C., Forster, P. M., Hargreaves, J. C., Hegerl, G., Klein, S. A., Marvel, K. D., Rohling, E. J., Watanabe, M., Andrews, T., Braconnot, P., Bretherton, C. S., Foster, G. L., Hausfather, Z., von der Heydt, A. S., Knutti, R., Mauritsen, T., Norris, J. R., Proistosescu, C., Rugenstein, M., Schmidt, G. A., Tokarska, K. B., and Zelinka, M. D.: An Assessment of Earth's Climate Sensitivity Using Multiple Lines of Evidence, Reviews of Geophysics, 58, e2019RG000 678, https://doi.org/10.1029/2019RG000678, 2020.

Sokol, A. B. and Hartmann, D. L.: Tropical Anvil Clouds: Radiative Driving Toward a Preferred State, Journal of Geophysical Research: Atmospheres, 125, e2020JD033 107, https://doi.org/10.1029/2020JD033107, 2020.

Sokol, A. B., Wall, C. J., and Hartmann, D. L.: Greater Climate Sensitivity Implied by Anvil Cloud Thinning, Nature Geoscience, pp. 1–6, https://doi.org/10.1038/s41561-024-01420-6, 2024.

Takahashi, H. and Luo, Z. J.: Characterizing Tropical Overshooting Deep Convection from Joint Analysis of CloudSat and Geostationary Satellite Observations, Journal of Geophysical Research: Atmospheres, 119, 112–121, https://doi.org/10.1002/2013JD020972, 2014.

Takahashi, H., Protopapadaki, S., Stubenrauch, C., Luo, Z. J., and Stephens, G. L.: Relationships between Convective Strength and Anvil Development Based on AIRS-CloudSat Joint Dataset, 2017.

Wall, C. J., Norris, J. R., Gasparini, B., Smith, W. L., Thieman, M. M., and Sourdeval, O.: Observational Evidence That Radiative Heating Modifies the Life Cycle of Tropical Anvil Clouds, Journal of Climate, 33, 8621–8640, https://doi.org/10.1175/JCLI-D-20-0204.1, 2020.

Williams, A. I. L. and Jeevanjee, N.: A Robust Constraint on the Response of Convective Mass Fluxes to Warming, Journal of Advances in Modeling Earth Systems, 17, e2024MS004 695, https://doi.org/10.1029/2024MS004695, 2025.